Journal of Surgical Research **99,** 53–60 (2001)
doi:10.1006/jsre.2000.6073, available online at http://www.idealibrary.com on IDEAL®

Nonlinear Analysis of Arterial Oscillated Flow in Experimental Stenosis and Microsurgical Anastomosis

Philippe May, M.D.,*,†,‡,[1] Olivier Gerbault, M.D.,†,‡ Claudine Arrouvel,† Marc Revol, M.D., Ph.D.,†,‡ Jean M. Servant, M.D., Ph.D.,†,‡ and Eric Vicaut, M.D., Ph.D.*

**Laboratoire d'Etude de la Microcirculation, Université Paris VII, Hôpital F. Widal, 200 rue du Fg St Denis, 75010 Paris, France; †Laboratoire de Microchirurgie Expérimentale, Université Paris VII, Faculté Villemin-St Louis, 10 rue de Verdun, 75010 Paris, France; and ‡Service de Chirurgie Plastique Reconstructrice et Esthetique, Hôpital Saint-Louis, 1 avenue Claude Vellefaux, 75475 Paris Cedex 10, France*

Submitted for publication July 24, 2000; published online May 7, 2001

Background. **Thrombotic vascular occlusion is one of the main complications that can occur during microsurgical anastomosis and is frequent when the blood becomes turbulent. The aim of this *ex vivo* study was to test the use of nonlinear mathematical tools to detect turbulence flow upstream and downstream of an arterial stenosis and of a microsurgical anastomosis technique in arteries with diameters in the range of microsurgical practice.**

Materials and methods. **Rat carotid arteries (0.8 to 1.2 mm diameter) were transferred to a flow chamber and perfused with Krebs solution. An oscillated vascular flow was initiated with a peristaltic pump and a transit time flowmeter was used to measure flow with two probes. An arterial stenosis was created by a ligature and progressively increased ranging from 0 to 95%. For each flow signal three nonlinear analytical procedures were applied: time-delayed procedures, correlation dimension, and computing of the largest Lyapunov exponent.**

Results. **Our results indicated that the level of turbulence flow is correlated with the area reduction stenosis. In the range of 60–95% area reduction stenosis, we noted an experimental increase of turbulence flow. We also founded that a classical end-to-end anastomosis technique induced an increase of the turbulence flow in comparison with a control artery.**

Conclusions. **Thus nonlinear analysis can be useful in characterizing the complexity of an oscillated flow in small arteries submitted to stenosis or microsurgical anastomosis and may have clinical uses in detecting high level turbulent flow after microsurgery.** © 2001 Academic Press

Key Words: **artery; chaos; correlation dimension; flow chamber; Lyapunov exponent; microsurgery; nonlinear dynamics; oscillated blood flow; stenosis; turbulence.**

INTRODUCTION

The avoidance of thrombotic vascular occlusions is a crucial problem for the vascular surgeon during and after microsurgical anastomosis. Unlike the quasilaminar oscillated regime observed in a rectilinear artery, an arterial stenosis or a microsurgical anastomosis generates a turbulent, chaotic blood flow, and therefore facilitates fast thrombosis of the intervention [1–4]. In addition, thrombotic growth increases the turbulence rate of the fluid regime [5, 6]. It would be useful to be able to predict more precisely the real effect of the quality and type of microsurgical anastomosis on blood hemodynamics not only in a quantitative but also in a qualitative manner and hence on the quality of tissue perfusion. Following early work on nonlinear dynamic systems by Poincaré, Lorenz defined the dynamic of a chaotic system as "sensitive to initial conditions." Regarding the analysis of blood flow dynamics Ruelle and co-workers [7, 8] demonstrated that hydrodynamic turbulence is associated with a chaotic behavior and cannot be adequately analyzed by Fourier analysis, requiring specific nonlinear mathematical tools for nonlinear analysis [see 9–13 for details on methods]. Reynold's number and Womersley number are more familiar concepts for surgical researchers. However, a large amount of recent re-

[1] To whom correspondence should be addressed at Laboratoire d'Etude de la Microcirculation, Université Paris VII, Hôpital F. Widal, 200 rue du Fg St Denis, 75010 Paris, France. Fax: 01 40 05 43 65. E-mail: philippe.may@lrb.ap-hop-paris.fr.

0022-4804/01 $35.00

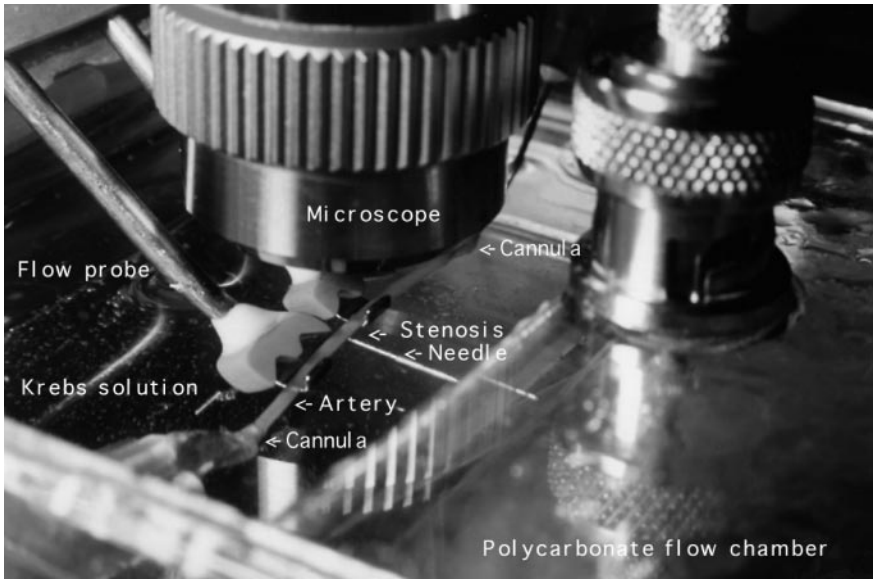

FIG. 1. Details of the polycarbonate flow chamber with the artery inside.

searcher has stressed that the use of other parameters are more adequate for characterizing turbulence in the case of pulsatile flow in a collapsible or viscoelastic tube [11, 14, 15]. The nonlinearity of a dynamic system means that some system variables, as well as their temporal derivatives, are coupled nonlinearly and are unpredictable. In such nonlinear dynamic systems a tiny difference in initial conditions of two trajectories grows exponentially with time. However, such unpredictable behavior does not exclude the presence of an underlying order, capable of analysis by nonlinear mathematical techniques. Computational methods are now available for characterizing and quantifying an apparently random experimental time series, thereby distinguishing deterministic chaos from stochastic noise [16, 17]. The correlation dimension and the largest Lyapunov exponent are the two parameters used to characterize the chaotic behavior of a turbulent system [7, 8, 10] and were used in this study [18, 19]. In medical physiology, Griffith and co-workers [20, 21] used these analytical procedures to observe the effects of specific pharmacological interventions on blood pressure and microcirculation vasomotion. Wagner and coworkers [22, 23] determined in the same way whether or not arterial blood pressure was governed by a chaotic control system. The aim of the present study was to test the use of nonlinear techniques for hydrodynamic microsurgical vascular research, to allow future estimation of the effect of different microsurgical techniques on microvascular hemodynamics [24]. To facilitate control of flow parameters and reduce homeostatic influences, we used rat carotid arteries perfused *ex vivo* in a flow chamber at constant pressure in order to evaluate the relationship between the level of turbulence and the degree of stenosis.

MATERIALS AND METHODS

Animal Preparation

Thirty wistar male rats weighing 350 to 450 g were chosen because of the similar scale of rat artery diameter and human artery diameter observed in microsurgery. Three groups of 10 rat carotid arteries were studied: In group 1, carotid arteries were used as control. In group 2, variable arterial stenosis from 0 to 90% was used. In group 3 we underwent standard end-to-end anastomosis with six stitches of 10.0 nylon. Animals were housed and cared for in accordance with our institution's guidelines. They were anesthetized intraperitoneally with 50 mg/kg sodium pentobarbital. Body temperature was maintained with a homeothermic blanket control unit (Harvard). The left cervical area was shaving with electric clippers and disinfected with betadine, and the cervical vasculature exposed via a longitudinal incision. The left carotid artery (0.8 to 1.2 mm in diameter) was then dissected atraumatically along its entire length. The proximal end of the artery was identified, to maintain the direction of the normal flow through the artery after mounting.

Perfusion System

A perfusion system based on that developed by Labadie *et al.* [25] was used (Fig. 1). The constant-flow head is generated by a pulsatile pump (Masterflex pump, Cole-Parmer Instrument Company, Chicago, IL). Perfusion frequency was maintained constant and the pulsatile rate was chosen to be 2 Hz as previously used by Low and Chew [26] in their study. Flexible silicone tubes were used (Silastic, No. 601-325/0.104 in. i.d., 0.192 in. o.d./HH109226/Dow Corning Corporation, Medical Products, Midland, MI). Perfusates were collected in a downstream reservoir, which served as both a sampling port and an inlet to the centrifugal pump. Thirty seconds after dissection, arteries were carefully and immediately transferred to the polycarbonate flow chamber containing Krebs solution, thermostated at 37°C, and oxygenated (95% O_2, 5% CO_2). The solution was constantly renewed to maintain the same pH and preserve physiological wall artery properties. The temperature inside and outside the chamber was controlled by a circular heating coil and continuously monitored by a thermistor probe (Digi-sense, thermocouple thermometer), inserted through the chamber wall and placed in the bath. The proximal and distal ends of the artery were secured to

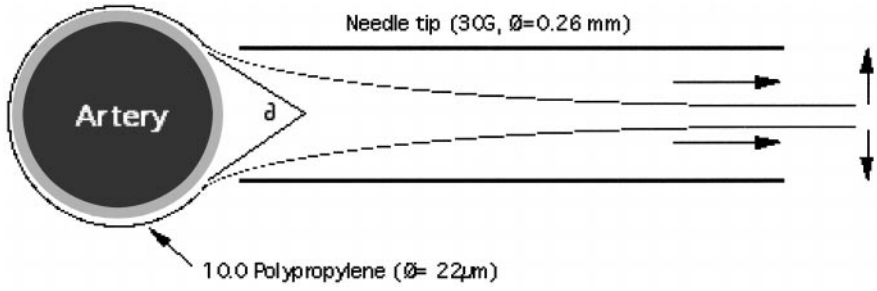

FIG. 2. Profile of the progressive arterial stenosis system used.

cannulas with cyanoacrylate glue. Axial length was fixed by viewing the vessel under a dissecting microscope and adjusted by positioning the distal cannula with the help of a micromanipulator (Prior Manipulators, Stoeling Co., IL). The flow chamber was placed on the stage of a microscope (Wild Leitz, Germany) and a video system (Video Camera CCD; VW-GL 350, Digital Panasonic, U.S.A.) to facilitate control of the stenosed area. Microsurgical 10.0 polypropylene was used for both variable stenosis and anastomosis (Fig. 2: side view). Reduction of the variable concentric area was analyzed with NIH Image Software (No. 1.62b7, National Institutes of Health, Bethesda, MD) and the percentage was expressed in area reduction: % stenosis = $100 \times [1 - (A2/A1)]$, where $A1$ was the cross-sectional area distal to the stenosis and $A2$ was the cross-sectional area within the stenosis. Standard end-to-end sutures were made with six stitches of 10.0 nylon. Flow probes were symmetrically positioned and carefully fixed close to the stenosed or anastomosed artery which had been bathed in the Krebs solution, provided as an acoustic coupling agent. Probe orientation was guided by the intensity of the flow signal. No manipulation of the probe itself was necessary after its initial orientation. To have an oscillated flow reference from the pulsatile pump, we studied in a preliminary experiment the oscillated flow generated through a Silastic noncollapsible tube with a diameter in range of the carotid artery ($N = 10$ experiments).

Measurements

The transit time flowmetry signal which is frequently used in microvascular research [25, 27–29] was applied to the detection of each signal. To compare the direct flowmetry measurements, before and after stenosis, the transit-time flowmeter (T206, Transonic Systems, Ithaca, NY) was used with a probe (Model IV, Transonic Systems) that was adjustable to the range of carotid diameter. Probes were precalibrated by the manufacturer and provided absolute flow. Fluid pressure was controlled both proximal and distal to the artery segment with fixed pressure transducers (Uniflow, Baxter Healthcare, Irvin, CA). The pressure transducers were directly fixed to the end of the cannulas as noted in the model by Labadie *et al.* [25]. At the beginning of all experiments, the system pressure was constant and measured at 99.1 ± 6.7 mm Hg. Flow and pressure were recorded via a personal computer equipped with an analog-to-digital data acquisition system (Model MP30, Biopac Systems, Inc., Santa Barbara, CA). The system was programmed with acquisition and linear analysis software (Biopac Student Lab Software, Inc., Santa Barbara, CA). Flow signals were passed through a 10 Hz (Transonic) filter and stored on a hard disk with a sampling frequency of 50 Hz, according to Shannon's signal theorem. Altogether, the analysis of one data set with 1024 data points required 30 s, according to Wagner and co-workers [22, 23]. We checked in the present study that signal-to-noise ratio for all flow signal recorded was of the order of 100.

Nonlinear Analytical Procedures

We used nonlinear analysis of the flow signal using specialized algorithms [16, 17]. This allowed us to characterize the level of turbulence [30] by the following parameters:

The return maps. The return map is a graphical representation of a dynamic process allowing visual differentiation of deterministic vs chaotic dynamics. They are depicted in (Fig. 3) for three different stenosis levels and show the increase in instability and in trajectory divergence.

The correlation dimension (Dc). The correlation dimension which is a measure of a system's complexity and constitutes the minimum number of independent variables involved in generating the dynamics of an irregular time series [16]. A value of $Dc > 2$ is the central argument required to classify irregular temporal events as chaotic.

Lyapunov exponents. These are direct measures of the predictability of the time course of a system. In a globally linear and stable system, all Lyapunov exponents are zero or negative, and no information is produced. If any of the Lyapunov exponents are positive, the linear system is unstable and is sensitive under initial conditions: this is the definition of a chaotic system of [31]. In this study, we chose to calculate the largest Lyapunov exponent. The positive value of this characterized the turbulence level [32], i.e., the instability of the arterial flow. Further details on the principles of these methods are given in the Appendix.

Statistical Analysis

Data are expressed as means ± SEM. Differences between groups were tested by non-parametric Mann-Whitney test and correlation between degree of stenosis and level of turbulence were evaluated by the nonparametric Spearman test for paired data. A P value of ≤ 0.05 was considered significant.

We used the method of surrogate data to test the null hypothesis that the data arise from a stochastic linear process and attempted to reject it by comparing the value of a nonlinear parameter taken on by the data with its probability distribution estimated by a Monte Carlo resampling technique [33].

RESULTS

Surrogate data. We applied the method of surrogate data and found the values of the nonlinear parameters for the original data and the surrogates to be significantly different.

Return maps. In the three groups, the largest Lyapunov exponents were positive, thus demonstrating that the flow dynamics were nonlinear and chaotic with respect to the conclusion of the surrogate data tests. The average correlation dimension of the oscillations was estimated at 2 to 3, thus implying that more

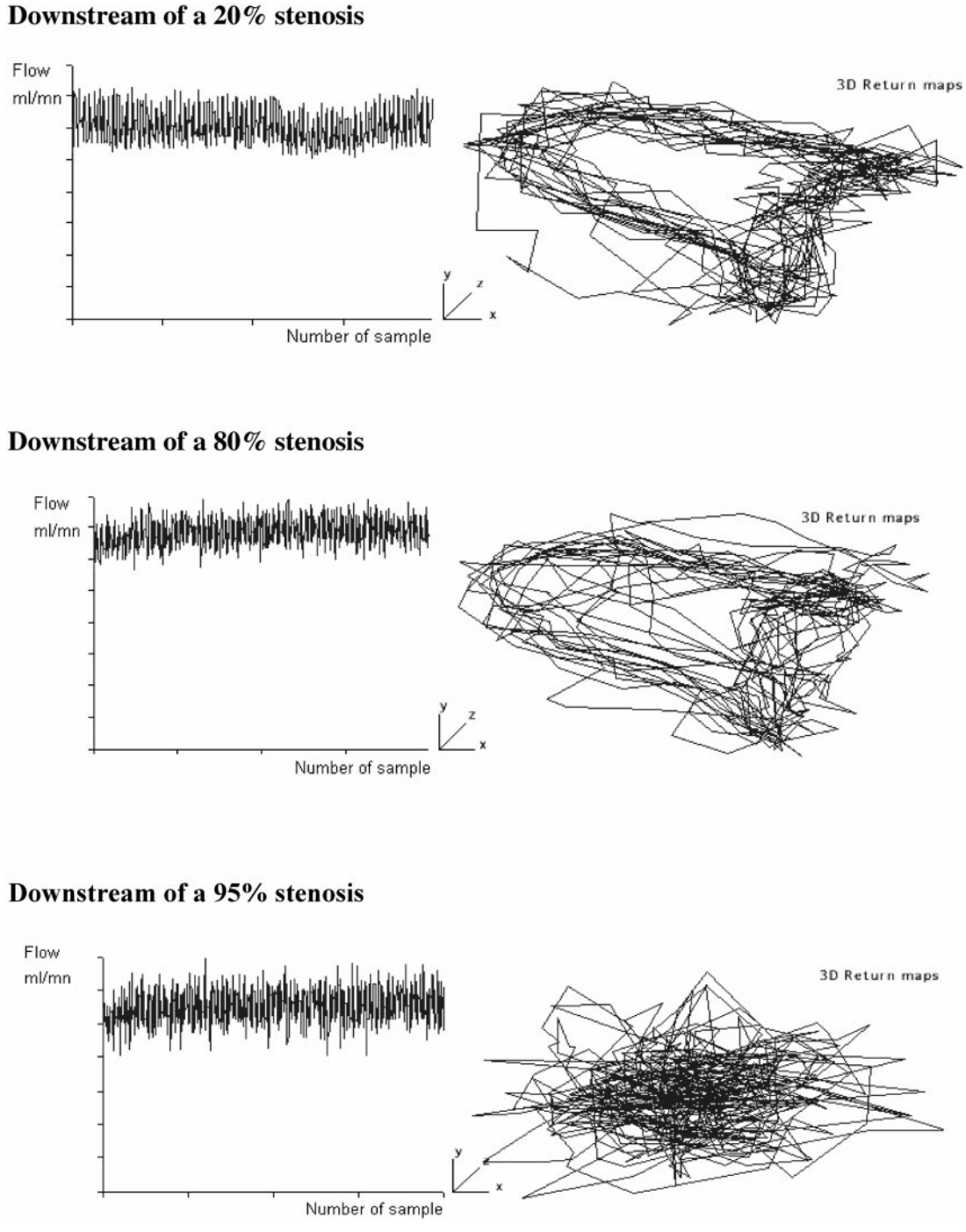

FIG. 3. Temporal evolution of the flow signal, and the corresponding return maps, in three different degrees of arterial stenosis.

than two independent control variables were necessary to account for the complexity of rat carotid artery dynamics.

Preliminary experiments: The Silastic noncollapsible tube. For the 10 recorded flow signals, the mean of the largest Lyapunov exponents was almost the same, at ≈0 bits/iteration (i.e., 0.04 ± 0.01). The correlation dimensions were ranged between 1 and 2 with a mean of 1.5 ± 0.07.

Group 1: Normal arteries (control). All the largest Lyapunov exponents were positive. For the 10 recorded flow signals, the mean of the largest Lyapunov exponents was 0.754 ± 0.05 bits/iteration, respectively. The correlation dimensions ranged between 2 and 3 with a mean of 2.6 ± 0.04.

Group 2: Progressive arterial stenosis. Visualizations of three carotid time flow series, corresponding to arteries with three different degrees of stenosis, are

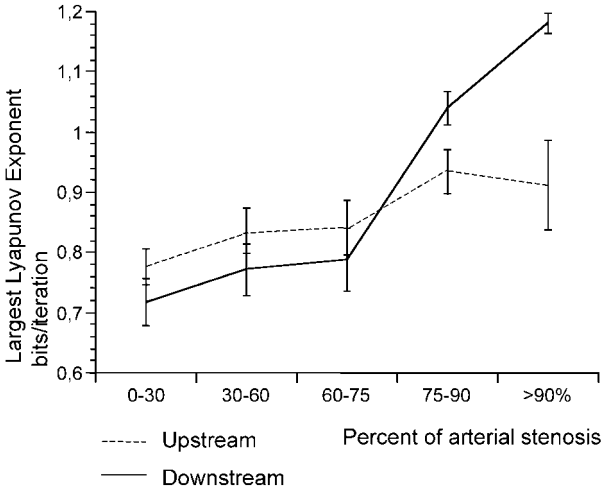

FIG. 4. Largest Lyapunov exponents expressed as means ± SEM in the case of progressive stenosis artery ($P < 0.005$).

shown in Fig. 3. The mean values (±SEM) of arterial diameter within the stenosis were for 0, 30, 60, 75, or 90% stenosis, respectively, 1 ± 0.035, 0.84 ± 0.029, 0.64 ± 0.022, 0.50 ± 0.017, or 0.32 ± 0.011 mm. The mean values (±SEM) of the largest Lyapunov exponents are shown in (Fig. 4) as an adjunct to graphic analysis of the system's state. The largest Lyapunov exponent, downstream of the stenosis, increased greatly after a 60% reduction in the stenosed area ($P < 0.005$). Note that as in the normal arteries, the largest Lyapunov exponent was positive for all the progressive stenosis signals and the correlation dimension estimations ranged between 2 and 3 ($P < 0.005$).

Group 3: End-to-end anastomosis technique. The correlation dimension was estimated at 2 to 3 and compared to the control arteries. There was a significant increase ($P < 0.005$) in the largest Lyapunov exponent values upstream and more downstream of the anastomosis. The use of six stitches of 10.0 nylon increased the turbulence regime upstream of the anastomosis and this effect was higher downstream (Fig. 5) in comparison with control carotid arteries ($P < 0.005$).

DISCUSSION

The concept of two-dimensional chaos has proved fruitful for the understanding of many complex phenomena. In contrast with the linear dynamics found in preliminary experiments in a noncollapsible tube several researcher [11, 12, 14] demonstrated that much of the complex dynamic behavior observed in a simple collapsible tube model is due to nonlinear dynamics. In the cardiovascular system, Parthimos and co-workers measuring time-dependent fluctuations of blood pressure and blood flow in isolated ear artery demonstrated how vasomotion may exhibit nonlinear chaotic behavior [34]. Recently, Griffith and Edwards used the nonlinear systems theory to show the high degree of variability in perfusion conditions in response to pharmacological interventions [35]. Similar methods were used by Bräuer and Hahn to characterize blood flux in human vessels measured by laser-Doppler fluxmetry in patients with Raynaud's phenomenon [36]. Here we tested the use of nonlinear techniques to quantify the level of the turbulence with diameters in the range of microsurgical practice. We used three analytical procedures for nonlinear dynamic systems in the hydrodynamic time series: The first was the return map, which describes the relation of a given point in the time series to the next point in the series, the points being separated by a given time delay. This allowed a powerful graphic representation of a given system of dynamics. However, the return map alone does not make it possible to distinguish between chaotic and stationary dynamics. Therefore, in the second and third procedures, we computed the correlation dimension and the largest Lyapunov exponent, to provide our system with dynamic complexity. In the three carotid rat artery groups studied here, all the largest Lyapunov exponents were positive and indicated a deterministic nonlinear chaotic system evolution. This means that the flow oscillations measured in an isolated rat carotid artery perfused by a pulsatile pump have a chaotic nature. In addition, using nonlinear flow signal analysis, we demonstrated the relationship between the increasing turbulence level and the increase in the reduction of the stenosed area. It should be noted that in the three groups of arteries studied here, the correlation dimension varied between 2 and 3. This suggests the involvement of at least three interdependent control variables [31]. These values were lower than those found by Wagner and Persson [22] for blood pressure or renal blood flow in conscious dogs but were

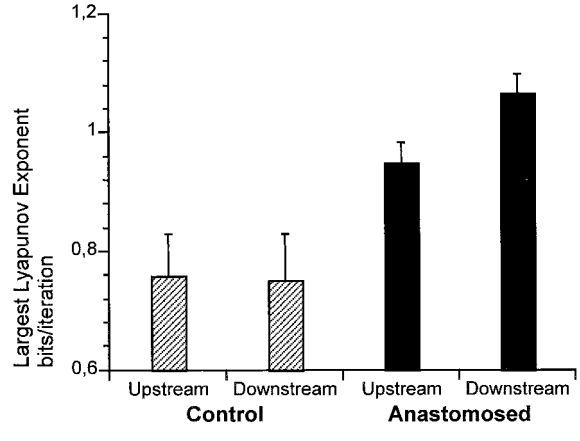

FIG. 5. Largest Lyapunov exponents expressed as means ± SEM in the case of control versus anastomosed arteries ($P < 0.005$).

similar to those found by Griffith and Edwards [21] when analyzing time series in an isolated rabbit ear artery 150 μm in diameter. In terms of degree of freedom these results could suggest a limit of three independent variables for an *ex vivo* physiological dynamical system. Garfinkel *et al.* [37] demonstrated that the sensitivity under initial conditions not only makes a dynamical system unpredictable but makes them extremely susceptible to control. Incorporating chaos into practical systems therefore yields a maximum flexibility in their performance. The increase of the largest Lyapunov exponent downstream of a 60% reduction in the rat carotid stenosed area observed here was in line with the well-known hemodynamics of the poststenotic flow in microsurgery and with the results obtained by Hutchison using spectral analysis downstream in an *in vivo* dog carotid artery [38] and was constant in the same range of 2 to 3, indicating the involvement of at least three control variables [31]. Although every approach has its individual pitfalls and limitations, all our results indicate that analytical techniques derived from the field of chaos theory can be useful in characterizing the stability and complexity of an oscillated fluid regime in small arteries submitted to stenosis. Since these methods allow determination of the level of turbulence generated by a surgical procedure, they can provide some information about the quality of anastomosis and may have important clinical uses in microsurgery. In the same way, it would be very interesting to observe the turbulence growth in an *in vivo* study. Further investigation is necessary to apply this mathematical protocol in an *in vivo* study and further investigation will be necessary to test the usefulness of such mathematical analysis used *in vivo* to characterize the degree of turbulence blood flow in a stenosis or an anastomosis.

APPENDIX

Brief Summary of Mathematical Methods Used in the Present Study

In general, the description of a deterministic system is concerned with the properties of its phase space or state space. A phase space is a coordinate system whose axes are defined by the independent variables of the system under study. In our case the system under study is the hemodynamics. Several years ago, a statistical description for a system with many degrees of freedom (thermodynamics) was introduced. Biological systems may have an almost infinite number of degrees of freedom but only a few are necessary to describe their behavior. Thus, relevant information concerning the whole system may be extracted from the observation of a single variable (blood flow, blood pressure, etc.). This signal contains information about the complete system, since all degrees of freedom are interwined. If the system is described by an ordinary differential flow the entire phase history is given by a smooth curve in phase space. Each point on this curve represents a particular state of the system at a particular time. For closed systems, no such curve can cross itself. If a phase history of a given system returns to its initial condition in phase space, then the system is periodic and it will cycle through this closed curve for all time.

In this study graphic representations and parameters of nonlinear dynamics were used in the following order.

Phase space representation or return map. Deterministic dynamical systems can be expressed for example by ordinary differential equations,

$$x'(t) = f(x(t))$$

or in discrete time

$$t = n\Delta t$$

by maps of the form,

$$x_{n+1} = f(x_n).$$

The return map of a dynamics system is a mathematical construction in which a different coordinate axis is assigned to each of the temporal variables needed to specify the system's instantaneous state. According to Taken's embedding theorem [7], the reconstructed dynamics in the form of a return map are geometrically similar to the original for both continuous-time and discrete-time systems. This mathematical construction is generated solely by the value of a single known temporal variable (for example, the transit time flow signal) and is useful for representing in our experimental research, the entire behavior of the dynamic flow system. The return map coordinates are determined by time-delayed values separated by a fixed time (τ), the time delay.

Time delay: τ. The most important phase space reconstruction technique is the method of delays. Vectors V_i in a new space, the embedding space, are formed from time delayed values of the scalar measurements:

$$\mathbf{V}_0 = \{x(0),\ x(\tau),\ x(2\tau),\ x(3\tau),\ \ldots,\ x[(m-1)\tau]\}$$

$$\mathbf{V}_1 = \{x(1),\ x(\tau+1),\ x(2\tau+1),\ x(3\tau+1),\ \ldots,\ x[(m-1)\tau+1]\}$$

$$\mathbf{V}_2 = \{x(2),\ x(\tau + 2),\ x(2\tau + 2),\ x(3\tau + 2),\ \ldots,\ x[(m-1)\tau + 2]\}$$

:

$$\mathbf{V}_i = \{x(i),\ x(\tau + 2),\ x(2\tau + i),\ x(3\tau + i),\ \ldots,\ x[(m-1)\tau + i]\}$$

The number m of elements is called the embedding dimension and the time τ is generally referred to as the delay. m is the smallest dimension that contains the attractor. Famous embedding theorems by Takens [30] state that the time-delay embedding provides a one-to-one image of the original set $\{x\}$, commonly referred to as an attractor.

Then it is possible to distinguish nonlinear dynamic systems from random processes by analyzing the phase space behavior of their trajectories. Totally random processes can completely fill up the return map, unlike periodic or chaotic processes. Examples of return maps are illustrated below.

White noise in a 2D-return map after plotting y versus x:

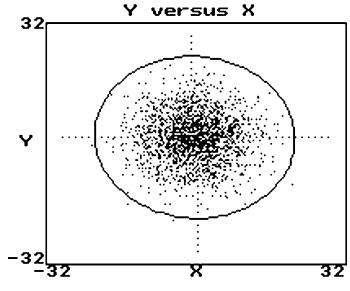

In periodic or chaotic processes, the trajectories are restricted to a bounded region in the return map, the attractor.

Lorenz attractor which is illustrated below in a 2D-return map after plotting y versus x:

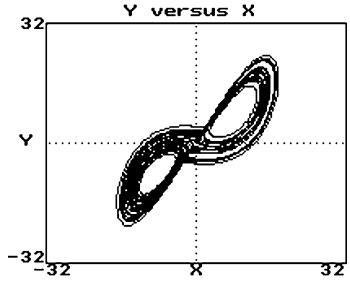

Lorenz attractor in a 3D-return map after construction of delay vectors $\mathbf{V}_i$:

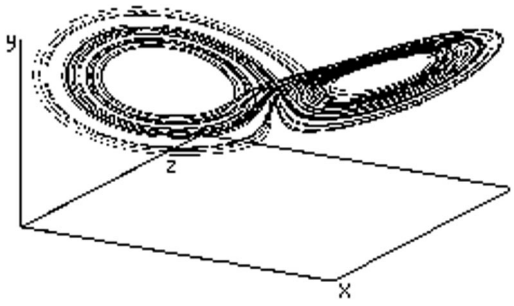

The best value of the time delay τ was determined by the first zero of the signal's autocorrelation function, to ensure the independence of each vector component. In our study for each flow signal the return map was embedded with the time-delayed values measured. Therefore the next step was the same for all flow signals in the three groups of arteries studied. It consisted of estimating the correlation dimension with the Grassberger-Procaccia algorithm, and then of computing the largest Lyapunov exponent with the fixed-time evolution program by Wolf *et al.* [17].

The correlation dimension (Dc). This is a measure of a system's complexity and constitutes the minimum number of independent variables involved in generating the dynamics of an irregular time series [16]. Usually, strange attractors have noninteger dimensions, and algorithms and methods exist to determine these dimensions. The Grassberger-Procaccia algorithm was applied here to estimate the correlation dimension of the time series, and 1024 points of the original time series were used according to Wagner and co-workers [22, 23]. A value of $\mathrm{Dc} > 2$ is the central argument required to classify irregular temporal events as chaotic.

Lyapunov exponents. These are direct measures of the predictability of the time course of a system. This is defined as the coefficient of the average exponential growth per unit time between the initial and final states of the system. In a globally linear and stable system, all Lyapunov exponents are zero or negative, and no information is produced. If any of the Lyapunov exponents is positive, the linear system is unstable and is sensitive under initial conditions: this is the definition of a chaotic system of [31]. An m-dimensional system has m Lyapunov exponents. In this study, we chose to calculate the largest Lyapunov exponent. The positive value of this characterized the turbulence level [32], i.e., the instability of the arterial flow. The fixed-time evolution program by Wolf *et al.* [17] was used to compute this nonlinear parameter.

The reader who would like further information on these methods can refer to the books of Kantz and Schreiber [9] and Kaplan and Glass [19].

ACKNOWLEDGMENTS

This work was carried out with support from La Fondation de l' Avenir and La Fondation pour la Recherche Médicale. We express our gratitude to them.

REFERENCES

1. Johnson, P. C., Dickson, C. S., Garrett, K. O., Sheppeck, R. A., and Bentz, M. L. The effect of microvascular anastomosis configuration on initial platelet deposition. *Plast. Reconstr. Surg.* **91:** 522, 1993.
2. Linden, M., Sirsjo, A., Lindbom, L., Nilsson, G., and Gidlof, A. Laser Doppler perfusion imaging of microvascular blood flow in rabbit tenuissimus muscle. *Am. J. Physiol.* **269:** H1496, 1995.
3. Moskovitz, M. J., Zhang, L., Baron, D. A., Kanner, B. J., Tuchler, R. E., and Siebert, J. W. Transient postoperative stenosis in small-vessel anastomoses. *Ann. Plast. Surg.* **34:** 309, 1995.
4. Asada, Y., and Sumiyoshi, A. Histopathology of thrombotic vascular diseases. *J. Clin. Med.* **57:** 1555, 1999.
5. Cloutier, G., Allard, L., and Durand, L. G. Changes in ultrasonic doppler backscattered power downstream of concentric and eccentric stenoses under pulsatile flow. *Ultrasound Med. Biol.* **21:** 59, 1995.
6. Padet, J. *Fluides en écoulement.* Paris: Masson, 1991. Pp. 99–279.
7. Ruelle, D., and Takens, F. On the nature of turbulence. *Commun. Math. Phys.* **20:** 167; **23:** 343, 1971; Newhouse, S., Ruelle, D., and Takens, F. Occurrence of strange Axiom A attractors near quasiperiodic flows on T^m, $m \geq 3$. *Commun. Math. Phys.* **64:** 35, 1978.
8. Ruelle, D. Strange attractors. *Math. Intell.* **2:** 126, 1980.
9. Kantz, H., and Schreiber, T. *Nonlinear Time Series Analysis.* Cambridge, UK: Cambridge Univ. Press, 1997. Pp. 29–171.
10. Manneville, P. *Structures dissipatives chaos et turbulences.* Aléa-Saclay, 1990. Pp. 1–361.
11. Pedley, T. J. Nonlinear pulse wave reflection at an arterial stenosis. *J. Biomech. Eng.* **105:** 353, 1983.
12. Roffeh, Y., Einav, S., Liaw, J., Whiting, J., and Keren, G. Cepstrum analysis of reflected pressure waves in stenosed arteries. *Med. Biol. Eng. Comput.* **34:** 175, 1996.
13. Sipkema, P., and Westerhof, N. Mechanics of a thin walled collapsible microtube. *Ann. Biomed. Eng.* **17:** 203, 1989.
14. Jensen, O. E. Chaotic oscillations in a simple collapsible-tube model. *J. Biomech. Eng.* **114:** 55, 1992.
15. Groisman, A., and Steinberg, V. Elastic turbulence in a polymer solution flow. *Nature* **405:** 53, 2000.
16. Grassberger, T., and Procaccia, I. Measuring the strangeness of strange attractors. *Phys. D* **9:** 189, 1983.
17. Wolf, A., Swift, J. B., Swinney, H. L., and Vastano, J. A. Determining Lyapunov exponents from a time series. *Phys. D* **16:** 285, 1985.
18. Glass, L., and Kaplan, D. Time series analysis of complex dynamics in physiology and medicine. *Med. Prog. Technol.* **19:** 115, 1993.
19. Kaplan, D., and Glass, L. *Understanding Nonlinear Dynamics.* New York: Springer-Verlag, 1995. Pp. 279–338.
20. Griffith, T. M. Temporal chaos in the microcirculation. *Cardiovasc. Res.* **31:** 342, 1996.
21. Griffith, T. M., and Edwards, D. H. Modulation of chaotic pressure oscillations in isolated resistance arteries by EDRF. *Eur. Heart J.* **14:** 60, 1993.
22. Wagner, C. D., and Persson, P. B. Nonlinear chaotic dynamics of arterial blood pressure and renal blood flow. *Am. J. Physiol.* **268:** H621, 1995.
23. Wagner, C. D., Nafz, B., and Persson, P. B. Chaos in blood pressure control. *Cardiovasc. Res.* **31:** 380, 1996.
24. Lee, B. Y., Thoden, W. R., Brancato, R. F., Kavner, D., Shaw, W., and Madden, J. L. Comparison of continuous and interrupted suture techniques in microvascular anastomosis. *Surg. Gynecol. Obstet.* **155:** 353, 1982.
25. Labadie, R. F., Antaki, J. F., Williams, J. L., Katyal, S., Ligush, J., Watkins, S. C., Pham, S. M., and Borovetz, H. S. Pulsatile perfusion system for ex vivo investigation of biochemical pathways in intact vascular tissue. *Am. J. Physiol.* **270:** H760, 1996.
26. Low, H. T., and Chew, Y. T. Pressure/flow relationships in collapsible tubes: Effects of upstream pressure fluctuations. *Med. Biol. Eng. Comput.* **29:** 217, 1991.
27. D'Almeida, M. S., Gaudin, C., and Lebrec, D. Validation of 1- and 2-mm transit-time ultrasound flow probes on mesenteric artery and aorta of rats. *Am. J. Physiol.* **268:** H1368, 1995.
28. Tuchler, R. E., Zhang, L., Siebert, J. W., and Shaw, W. W. Simultaneous comparison of pre- and post-microanastomotic hemodynamic profiles using a tandem doppler probe. *Microsurgery* **12:** 35, 1991.
29. Welch, W. J., Deng, X., Snellen, H., and Wilcox, C. S. Validation of miniature ultrasonic transit-time flow probes for measurement of renal blood flow in rats. *Am. J. Physiol.* **268:** F175, 1995.
30. Takens, F. *Detecting Strange Attractors in Turbulence. Lecture Notes in Mathematics.* New York: Springer, 1981. Vol. 898, pp. 366–381.
31. Abarbanel, H. D. I. *Analysis of Observed Chaotic Data.* New York: Springer-Verlag, 1996.
32. Baker, G. L., Gollub, J. P., and Blackburn, J. A. Inverting chaos: Extracting system parameters from experimental data. *Chaos* **6:** 528, 1996.
33. Theiler, J., Eubank, S., Longtin, A., Galdrikian, B., and Farmer, J. D. Testing for nonlinearity in time series: The method of surrogate data. *Phys. D* **58:** 77, 1992.
34. Parthimos, D., Edwards, D. H., and Griffith, T. M. Comparison of chaotic and sinusoidal vasomotion in the regulation of microvascular flow. *Cardiovasc. Res.* **31:** 388, 1996.
35. Griffith, T. M., and Edwards, D. H. Integration of non-linear cellular mechanisms regulating microvascular perfusion. *Proc. Inst. Mech. Eng. [H].* **213:** 369, 1999.
36. Bräuer, K., and Hahn, M. Nonlinear analysis of blood flux in human vessels. *Phys. Med. Biol.* **44:** 1719, 1999.
37. Garfinkel, A., Spano, M. L., Ditto, W. L., and Weiss, J. N. Controlling cardiac chaos. *Science* **257:** 1230, 1992.
38. Hutchison, K. J. Doppler ultrasound spectral shape downstream of significant arterial stenosis *in vivo. Ultrasound Med. Biol.* **21:** 447, 1995.